



---

# 1 Introduction

Over millions of years, nature has evolved unique processes, principles, materials, and structures which are excellently adapted to their function<sup>1–3</sup>. Consequently, mankind started early to use natural products for building and manufacturing of tools<sup>1,2</sup> or to draw inspiration for new technologies with one of the best known early examples being da Vinci's studies on the flight of birds<sup>4</sup>. Nowadays, interest in natural materials reaches so far that even governmental committees convened on the topic<sup>5</sup>.

During the past decades, study and imitation of natural processes, principles, materials, and structures has become a field of research on its own, known as bionics, bio-mimetics, or bio-inspiration<sup>2,6–10</sup>. The three terms are not clearly distinguished in literature and often used synonymously<sup>10–14</sup>. Among them, bio-inspiration is the most general term that just describes a broad idea or consideration of a principle from nature that led to an engineering application. As the most general term, bio-inspiration will be used as a superset of bio-mimetics and bionics to simplify readability in the following.

## 1.1 Examples for Bio-Inspiration in Engineering

Material science in particular has seen diverse examples for bio-inspired developments.

Fish scales and turtle carapace act as guides for the development of novel flexible armor systems<sup>15–17</sup> where, by architecture, they do not hinder motion but still offer protection by continuous overlaps (as in historical scale armor). Furthermore, as a consequence of interlocking joints (see **figure 1.1a**), turtle carapace even stiffens during strong deformation which prevents bruising of soft tissue in the event of an attack while the joints remain flexible during regular body motion.<sup>17</sup>

As another example, spider silk with its extreme specific strength and toughness<sup>18–20</sup> acts as a guide to develop synthetic fibers showing similarly advanced properties<sup>19,21–23</sup>. Furthermore, the characteristic to collect dew and the ability to



drain it off by the structure-driven formation of droplets (**figure 1.1b**) led to functional applications for water collection in dry environments as well <sup>24,25</sup>.

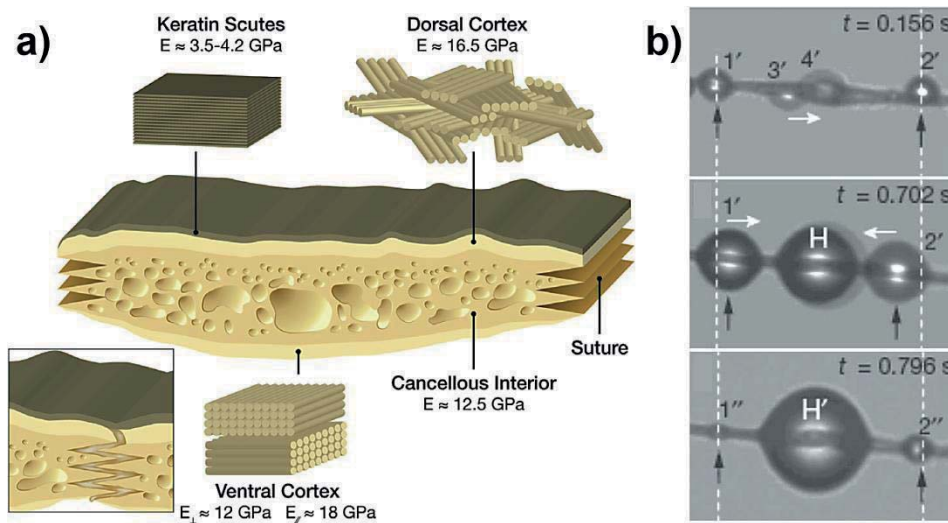


**Figure 1.1: Structure of turtle carapace (left) and water collection on spider silk (right).**

Left: The schematic shows the design principle of elements of the turtle carapace including the flexible suture joints (inset). <sup>17</sup> Right: Time resolved motion of water droplets toward each other on a strand of spider silk. Large droplets eventually detach and can be collected. <sup>25</sup> Reprinted with permission from Elsevier (left) and John Wiley & Sons (right).

Bone is known to provide structural integrity to the human body and that of other mammals and birds. To achieve this, it is simultaneously strong, stiff, and tough in order to avoid fracture and bending <sup>26–28</sup>. In addition, bone needs to be light not to hinder motion by inertia. Consequently, its buildup consists of varying combinations of a solid shell (cortical bone) and a spongy center (cancellous bone), see **figure 1.2a** <sup>3,26,27,29</sup>. This way, bone possesses high specific properties by tubular design that are similarly used in, e. g., lightweight frameworks <sup>29</sup>. The high specific properties are also the reason for research on synthetic material structures inspired by bone <sup>30–33</sup>.

Being mechanically strong and an optical wave guide at the same time, spicules from the marine sponge *Euplectella* (**figure 1.2b**) are examples for multi-functional natural composites. The spicules, acting as soil anchorage or skeleton back-bone <sup>3</sup>, consist of 99 vol% (volume percent) concentrically aligned silica layers bonded by interlayers of bio-polymers (1 vol%, **figure 1.2c**). This structure is extremely stiff and strong while weak interlayers and interphases cause crack deflection und thus toughening



with respect to monolithic silica.<sup>34–37</sup> This lamination also inspired multilayered all-ceramic composites<sup>38–40</sup>: By lamination of ceramic layers with tailored weak or strong inorganic interfaces, several research groups developed composites that are indeed simultaneously strong and tough<sup>41–47</sup>. Less explored but still promising is the work on organic-inorganic laminates with low fractions of organics<sup>39,40</sup>. The materials are tougher than their purely inorganic counterparts and they can reach similar strength and modulus<sup>39,40</sup> but thermal instability of the inorganic limits application. Due to its concentric layered arrangement and elongated structure sponge spicules also act as optical wave guides. Light is totally reflected, collected, and guided along the spicule, comparable to fiber optics<sup>48–50</sup>. Thus sponge spicules are not only inspiration for mechanical but also for optical applications as well as combinations of both.

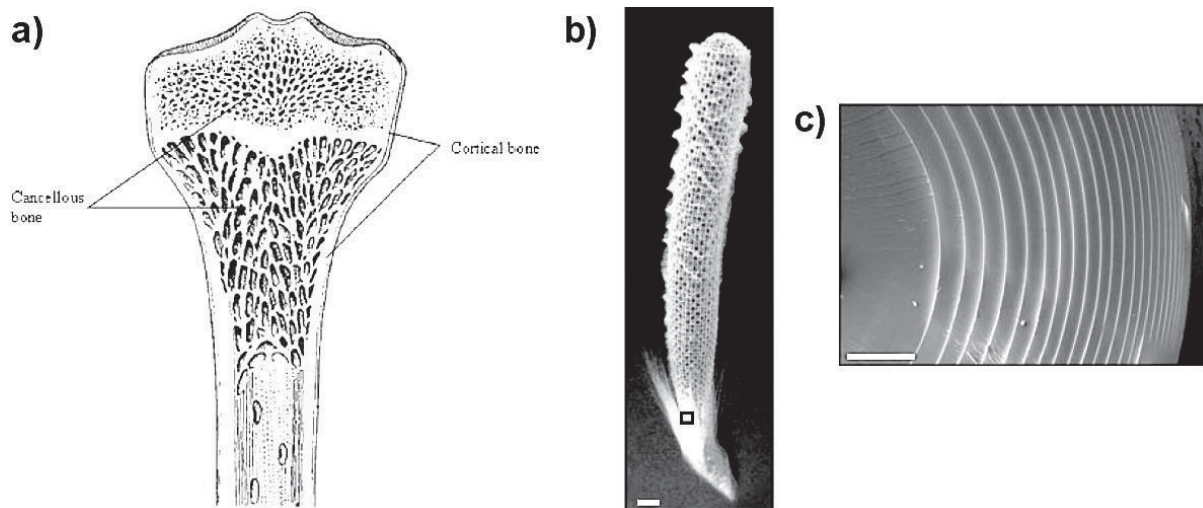


**Figure 1.2: Architecture of bone and sponge spicules.** a) Schematic representation of a longitudinal section of a femur bone. It shows the dense cortical bone around cancellous (spongy) bone in the center. In the bottom part, the hollow shaft is indicated.<sup>51</sup> Reprinted with permission from the Oxford University Press. b) Mineral skeleton of the marine sponge *Euplectella* with anchoring spicules at its base (black rectangle). Scale bar: 1 cm.<sup>35</sup> c) Concentrically laminated microstructure of *Euplectella* anchoring spicules with silica (dark) and polymeric (light) phases. Scale bar: 5  $\mu\text{m}$ .<sup>35</sup> (b) and (c) reprinted with permission from AAAS.

Spider silk, bone, and sponge spicule have in common that they combine high strength and high toughness – properties that are generally mutually exclusive<sup>52</sup>. This is reasoned by specialized structural designs which are also present in nacre, mother-of-pearl, the inspiration for this doctoral thesis.



## 1.2 Nacre, Mother-of-Pearl

Nacre, mother-of-pearl, is the innermost layer of several marine mollusk shells<sup>3,53,54</sup> (see **figure 1.3**). Its microstructure, microscopically investigated since the early 1950s<sup>55</sup> with first references dating back to 1930<sup>56</sup>, mainly consists of brittle aragonite, a polymorph of calcium carbonate (the basis of chalk), and mechanically rather weak bio-polymers<sup>53,54</sup>. However, a specific so-called brick-and-mortar-like microstructure leads to remarkable mechanical properties including high strength and high toughness simultaneously<sup>53,54</sup>, a combination hardly achieved in synthetic materials<sup>52,57</sup>. They are extremely interesting since neither the mineral nor the organic phase could provide them all alone. Their microstructural interplay is essential to achieve the mechanical performance as a composite<sup>53,58,59</sup>.

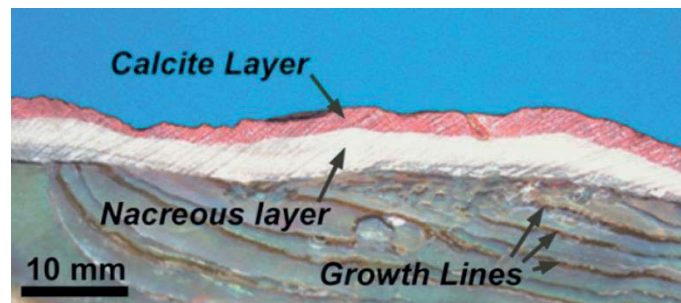


**Figure 1.3: Macroscopic structure of the shell of red abalone.** Monolithic prismatic calcite forms the outer layer while nacre can be found on the inside.<sup>53</sup> Reprinted with permission from Elsevier.

### 1.2.1 Composition and Microstructure of Nacre

Found in many different species, structure and properties of nacre vary broadly<sup>54</sup>. Aragonite, a crystallographic form of calcium carbonate ( $\text{CaCO}_3$ ), is located in polygonal tiles measuring 300 to 1000 nm in thickness and 4.5 to 8  $\mu\text{m}$  in diameter<sup>60,61</sup> with aspect ratios (diameter to thickness) between 9 and 14<sup>60</sup>. The tiles are arranged in staggered parallel layers and individually surrounded by 20 to 30 nm thick films of polysaccharides, proteins, and water. On the nanoscale, each tile in turn consists of roughly spherical mineral crystallites which are again separated and linked by even thinner layers of the organics. Considering the overall mineral fraction in nacre, literature is inconsistent with some publications referring to 95 vol% of aragonite<sup>53,62–65</sup> and some stating 95 wt%<sup>3,54</sup>. The remaining content is shared by bio-polymers and water. Although those values differ significantly due to a considerable difference in mass density of mineral and organic phases, the



inconsistency is not yet resolved. Anyway, the content of mineral in nacre is considerably higher than in commercially available ceramic-based synthetic materials<sup>63</sup>. The density of nacre amounts to  $2.7 \text{ g/cm}^3$ <sup>63</sup>. Depending on the species, overlaps between tiles of adjacent layers are either random or highly uniform. The latter leads to so-called columnar nacre based on columns of tiles with overlapping area fractions of about 66%. The former is called sheet nacre with less mean overlap.<sup>3,53,54,64</sup>

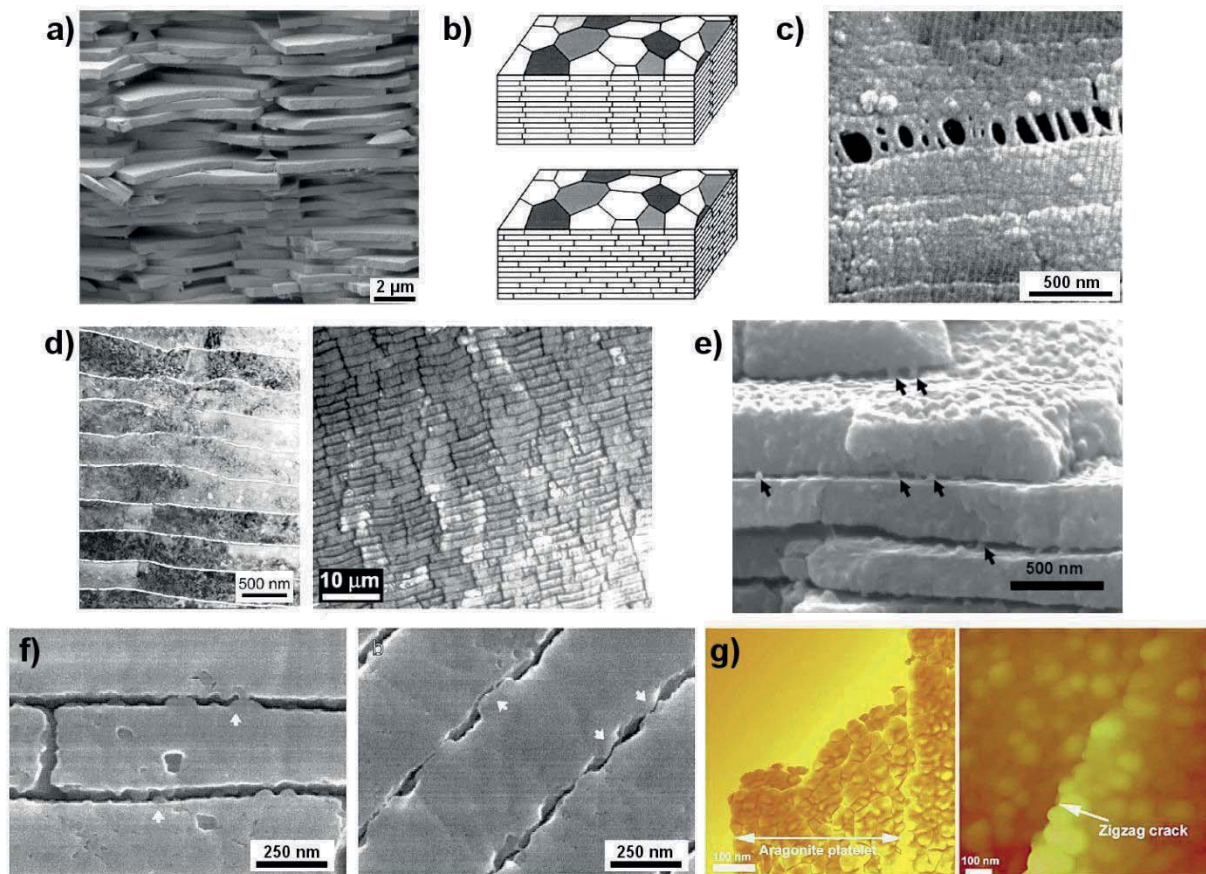


**Figure 1.4: Structural features of nacre on all length scales.** a) The arrangement of aragonite tiles in parallel layers.<sup>66</sup> b) Schematic illustration of columnar (top) and sheet nacre (bottom).<sup>67</sup> c) Polymer fibrils bridging a crack in nacre.<sup>62</sup> d) Waviness of tiles and layers on the meso-scale.<sup>53</sup> e) Mineral bridges (black arrows) between and nano-roughness on aragonite tiles in nacre.<sup>68</sup> f) Deformed nano-roughness (white arrows) in nacre.<sup>67</sup> g) Nano-crystallinity in aragonite tiles, indicated by surface topology (left) and the roughness of a crack surface (right).<sup>69</sup> Reprinted under Creative Commons CC-BY license by the Nature Publishing Group (a, g) and with permission from the Cambridge University Press (b, f), The Royal Society Publishing (c), Elsevier (d), or Dr. Albert Yu-Min Lin (e).



Due to its structural similarity to brick walls, the microstructure of nacre is frequently called a brick-and-mortar structure. This term appropriately describes the structure on the microscale but fails to incorporate multiple other features. In particular, there is a waviness to every mineral tile on the meso-scale, a nano-roughness on their surfaces, nano-sized mineral bridges connecting tiles perpendicular to their surfaces, and the nano-crystallites that form the tiles.<sup>3,53,54,70</sup> All six structural features of nacre – parallel arrangement, composite nature, layer waviness, nano-roughness, mineral bridges, and nano-crystallites – are summarized in **figure 1.4**.

Although the growth mechanisms of natural nacre are the basis of all microstructural features, growth of nacre will not be treated here to keep this thesis concise. Interested readers are instead kindly referred to corresponding literature by Meyers *et al.*<sup>3</sup>, Sun & Bhushan<sup>54</sup>, Zhang & Xu<sup>71</sup>, and others<sup>72–76</sup>. More interesting in the scope of this work are the mechanical properties that are closely related to the microstructure.

## 1.2.2 Mechanical Properties of Nacre

Mechanical properties of nacre are generally as diverse as the number of mollusk species producing it. Furthermore, the mechanical behavior of nacre has not only been investigated for different species but also in dry and wet condition as well as perpendicular and parallel to the major plane of the tiles. Consequently, a vast amount of data has been published to date.

To limit this amount of data, it will be reduced with respect to the intention of this thesis. Thus, focus will be set on the naturally occurring conditions for nacre in (a) wet state and (b) loading in tension along the tiles. Loading situations with tensile stresses along the tiles are the mechanically most preferable natural ones as the following literature review and theoretical considerations in later parts of this work will show.

The most comprehensive review of the mechanical properties of nacre has been provided by Sun & Bhushan<sup>54</sup> in 2012. This comprehensiveness extends over wet, dry, and fresh condition, loading parallel and perpendicular to the plane of tiles, and 14 different nacre-producing species. In absolute values, nacre is among the stiffest, strongest, and toughest natural materials<sup>77,78</sup> and its mechanical properties are even



better than those of several synthetic ceramic-based composites<sup>63</sup>. Its mass specific modulus is also quite remarkable while the specific strength is rather moderate<sup>77,78</sup>. Considering all species and various references<sup>3,53,54,60,61,63,67,79,80</sup> but only wet or fresh samples and only tensile (or compressive) loads parallel to the tiles, the mechanical performance of nacre can be summarized as indicated in **table 1.1**.

**Table 1.1: Summary of mechanical properties of nacre.** Data is limited to wet or fresh samples and loading parallel to the major plane of the aragonite tiles in nacre.

Modulus	60 to 140 GPa (mean around 60 to 80 GPa)	<sup>54</sup> 53,54,79
Poisson's ratio	0.4 prior to interlaminar sliding negative afterward	53,79
Micro-hardness	2.7 to 11.4 GPa	<sup>54</sup>
Nano-hardness	about 4 GPa	<sup>54</sup>
Tensile strength	35 to 140 MPa (mean around 60 to 80 MPa)	<sup>54,61</sup> 54
Tensile yield strength	60 to 70 MPa	53,79
Bending strength	230 to 275 MPa	63,67
Compressive strength	235 to 548 MPa	<sup>54</sup>
Shear strength	30 to 37 MPa	<sup>54</sup>
Strain at failure	0.5 to 0.8 %	61,79
Toughness (increasing R-curve)	0.1 to 1.65 kJ/m <sup>2</sup> rarely up to 13 kJ/m <sup>2</sup>	<sup>60,61,63,79</sup> 80
Fracture toughness	4 to 10 MPa√m	54,63,79

Using tensile tests, first comprehensive studies with respect to the variety in properties and species have been undertaken by Currey<sup>61</sup> in 1977. He reported a slightly viscoelastic deformation behavior with some plasticity and strains at failure around 0.5 %. Strength scatters for different species and corresponding thicknesses of aragonite tiles (0.3 to 1.5 μm) and can reach values between 35 and 116 MPa. In the meantime, toughness data go up to 1.65 kJ/m<sup>2</sup> for tension along and 0.15 kJ/m<sup>2</sup> for tension perpendicular to the tiles. According to Currey, all tests were done with wet samples that had been dry at some stage during processing.<sup>61</sup>

Results from Jackson *et al.*<sup>62,63</sup> on the species *Pinctada* (pearl oyster<sup>54</sup>) even go up to 140 MPa strength in tension<sup>62</sup> and 275 MPa in three-point-bending<sup>63</sup> while



toughness measured in three-point-bending on single-edge notched beams (SENB) just reaches  $1.24 \text{ kJ/m}^2$ , corresponding to  $4 \text{ to } 5 \text{ MPa}\sqrt{\text{m}}$ <sup>63</sup> fracture toughness. Furthermore, Jackson *et al.*<sup>63</sup> report bending moduli around  $60 \text{ GPa}$ . Wang *et al.*<sup>67</sup> basically confirmed these data but obtained slightly lower bending strength of about  $230 \text{ MPa}$ . It has to be mentioned, though, that the latter resulted from four-point bending with a larger volume under maximum stress compared to three-point bending. Hence, the probability to find critical defects in the stressed volume also increases which leads to more frequent early failure.<sup>59</sup>

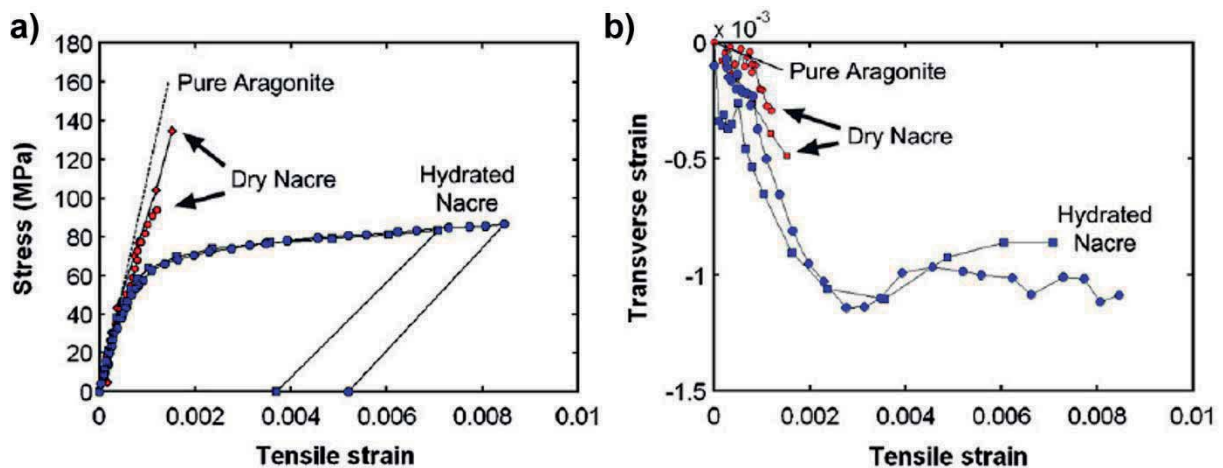


**Figure 1.5: Tensile stress (a) and transverse strain (b) over tensile strain from tests on nacre.** Dry nacre is almost as stiff and strong as monolithic (pure) aragonite and stronger but much more brittle than its hydrated form (a). In transverse direction, the samples first contract before they slightly expand again (negative Poisson's ratio). Eventually, the transverse strain assumes a steady state (vanishing Poisson's ratio).<sup>53</sup> Reprinted with permission from Elsevier.

In a more phenomenological investigation targeting acting deformation and fracture mechanisms (see **section 1.2.4**), Barthelat & Espinosa<sup>79</sup> also used tensile tests and three-point-bending on SENB and calculated a Young's modulus of  $80 \text{ GPa}$ ,  $60 \text{ MPa}$  yield strength followed by strain hardening and more than  $0.8 \%$  strain at failure. During deformation, Poisson's ratio first amounts to positive but eventually to negative and vanishing values, *i. e.* partially transvers expansion instead of contraction for lateral tension (see **section 1.2.4** and **figure 1.5**).<sup>53,79</sup> A typical stress-strain curve from corresponding experiments is shown in **figure 1.5**. Furthermore, they confirmed that nacre shows an *R*-curve behavior with initial and terminal toughness' around  $0.3$  and  $1.5 \text{ kJ/m}^2$  ( $4$  to  $10 \text{ MPa}\sqrt{\text{m}}$ ), respectively<sup>79</sup>. Dry





samples of nacre are generally stronger but more brittle and roughly as tough as their wet or fresh counterparts.<sup>54,62</sup>

In summary, typical tensile properties of wet nacre can be approximated as 100 GPa modulus, 100 MPa ultimate strength, and 10 MPa  $\sqrt{\text{m}}$  fracture toughness.

### 1.2.3 Mechanical Properties of the Constituents of Nacre

Nacre is a natural composite material. For the understanding of its mechanical performance and for accurate modelling, knowledge about the properties of the constituents is needed. Here, the term constituents will be understood in an effective sense that includes not only (inorganic) particles or tiles and (organic) matrix but also the interface that needs to be considered as an isolated volume. This is in agreement with cohesive zone models<sup>81</sup> and many approaches to model nacre-like materials<sup>82–84</sup> in which the weakest behavior of matrix and interface has to be accounted for. The topic will also be revisited later.

The aragonite tiles are characterized with a Young's modulus between 62.5 GPa<sup>85</sup> and 79 GPa<sup>86</sup>, a tensile strength ranging from 2.5 GPa<sup>86</sup> to 2.7 GPa<sup>85</sup>, and a toughness averaging at 1 to 3 J/m<sup>2</sup><sup>86,87</sup>. Hence, they are stronger but less tough than the composite nacre. A modulus of 79 GPa is more likely since established rules of mixture require it to be higher than the composite modulus indicated in **table 1.1** (see **section 2.1.2**).

Through the nano-roughness and waviness of tiles and the mineral bridges between them, interactions between two tiles and between tiles and matrix are believed to happen not only by adhesion but also by positive locking and continuous stiff bridging<sup>53,54</sup>. Consequently, modeling of the transfer of stresses cannot be broken down to shearing at the interface between organic and inorganic alone but additionally has to account for the other physical interactions mentioned above:

Katti *et al.*<sup>88</sup> measured the stiffness of cleaved surfaces of nacre and calculated a modulus of 20 MPa. Barthelat *et al.*<sup>86</sup> on the other hand attempted to characterize the organic matrix layer by nano-indentation and they obtained a modulus around 2.84 GPa, much higher than the former results. Due to the way of analysis, the modulus from Katti *et al.* is believed to be closer to the behavior of the neat matrix



material<sup>86</sup> while values of 2.8 to 15 GPa are actually repeatedly reported for the modulus of elasticity of the so-called interface region as a whole, *i. e.* the region between tiles including matrix material, nano-roughness, and mineral bridges<sup>54,65,85,86</sup>. Shear strength and toughness of the interface region are supposed to be strongly influenced by waviness, nano-roughness, and mineral bridges (see **section 1.2.4**). Consequently, it makes sense to state strength and toughness for the interface region as a whole and not for interface and matrix simultaneously. The shear strength was determined at approximately 30 MPa<sup>64,89</sup> while toughness data range from 1 J/m<sup>2</sup> to 5.5 J/m<sup>2</sup><sup>90</sup>.

Hence, neither the mineral tiles nor the matrix or interface alone provide the toughness in nacre (0.3 to 1.5 kJ/m<sup>2</sup>). They are actually all two to three orders of magnitude less tough. It is rather the interplay of interface region and tile arrangement that accounts for deformability and toughness while maintaining strength and stiffness of the mineral phase.

#### 1.2.4 Deformation Mechanisms and Fracture Mechanics of Nacre

*For this section, a basic knowledge of fracture mechanics is required and presumed. Section 2.1.1 may be consulted first, if these basics need to be complemented.*

To understand the origin of the mechanical properties of nacre, it is absolutely essential to know how nacre deforms and fractures. The basic access to all deformation mechanisms and fracture mechanics associated with nacre lies in its micro-structure and the mechanical behavior of its constituents and structural features. It is generally accepted that the deformability of nacre originates in interlaminar shearing of its tiles against each other, facilitated by a deformable organic matrix<sup>67,79</sup>. For small deformations, this process is fully elastic. For larger deformations, however, vertical matrix layers and interfaces fail. This failure of vertical matrix regions is highly delocalized and happens in several locations simultaneously as shown in **figure 1.6a** and **b**.<sup>67,79</sup> Still restricted to regions with highest stresses, this leads to the irreversible formation of process zones and dilatation bands in front of crack tips under load (see **figure 1.6c-f**)<sup>60,67,79</sup>, comparable to crazes in polymers<sup>61</sup>. This highly delocalized micro-cracking in process zones in front of stressed crack tips plays a major role in the toughening of